



Article

# A Common Target of Nitrite and Nitric Oxide for Respiration Inhibition in Bacteria

Wei Wang, Jiahao Wang, Xue Feng and Haichun Gao \*

Institute of Microbiology, College of Life Sciences, Zhejiang University, Hangzhou 310058, China

\* Correspondence: haichung@zju.edu.cn; Tel.: +86-571-8898-1107

**Abstract:** Nitrite and nitric oxide (NO) are well-known bacteriostatic agents with similar biochemical properties. However, many studies have demonstrated that inhibition of bacterial growth by nitrite is independent of NO. Here, with *Shewanella oneidensis* as the research model because of its unusually high cytochrome (cyt) *c* content, we identify a common mechanism by which nitrite and NO compromise cyt *c* biosynthesis in bacteria, and thereby inhibit respiration. This is achieved by eliminating the inference of the cyclic adenosine monophosphate-catabolite repression protein (cAMP-Crp), a primary regulatory system that controls the cyt *c* content and whose activity is subjected to the repression of nitrite. Both nitrite and NO impair the CcmE of multiple bacteria, an essential heme chaperone of the System I cyt *c* biosynthesis apparatus. Given that bacterial targets of nitrite and NO differ enormously and vary even in the same genus, these observations underscore the importance of cyt *c* biosynthesis for the antimicrobial actions of nitrite and NO.

**Keywords:** cytochrome *c*; cytochrome *c* biosynthesis; nitrite; nitric oxide; respiration



**Citation:** Wang, W.; Wang, J.; Feng, X.; Gao, H. A Common Target of Nitrite and Nitric Oxide for Respiration Inhibition in Bacteria. *Int. J. Mol. Sci.* **2022**, *23*, 13841. <https://doi.org/10.3390/ijms232213841>

Academic Editor: Tzong-Shyuan Lee

Received: 29 October 2022

Accepted: 8 November 2022

Published: 10 November 2022

**Publisher's Note:** MDPI stays neutral with regard to jurisdictional claims in published maps and institutional affiliations.



**Copyright:** © 2022 by the authors. Licensee MDPI, Basel, Switzerland. This article is an open access article distributed under the terms and conditions of the Creative Commons Attribution (CC BY) license (<https://creativecommons.org/licenses/by/4.0/>).

## 1. Introduction

Cytochromes *c* (cyts *c*), ubiquitous heme-containing proteins present in all domains of life, are essential for respiration and photosynthesis [1]. This type of protein is characterized by the covalent thioether bonds between the two cysteine residues within a heme-binding motif (HBM) (typically CXXCH, where X represents any amino acid residue) of apocytochrome (apocyt) and the two vinyl groups of the heme [2]. Multiple enzymatic complexes, called cyt *c* biosynthesis systems, are known to catalyze the formation of the bond [3]. Among them, System I, also called the cyt *c* maturation (CCM) system, found in diverse Gram-negative bacteria and archaea, as well as in plant and protozoan mitochondria, is no doubt the most complex and has been extensively studied in certain Gram-negative bacteria [2–6].

System I is composed of up to nine protein components, which form two functional modules, CcmABCDE for heme transport and delivery and CcmFGH(I) for disulfide reduction and heme-apocyt *c* ligation [2,7]. In Gram-negative bacteria, cyt *c* biosynthesis occurs entirely in the periplasm, requiring both the apocyt *c* and heme *b* molecules, which are translated and synthesized, respectively, in the cytoplasm and, subsequently, transported across the inner membrane (IM). While the translocation of apocyt *c* is a CCM-independent process carried out by the general secretion system, the CcmABCD complex mediates the transport of heme *b* into the periplasm. As a periplasmic heme chaperone, CcmE receives the heme from CcmABCD and subsequently passes it to the CcmFGH(I) module [8–11]. During heme transport, heme is attached to CcmE through a single covalent bond between a histidine (H130 in CcmE of *Escherichia coli*) and a vinyl group of heme [12,13]. Both the apocyt *c* and heme *b* molecules are eventually loaded onto the CcmFGH(I) module for ligating heme to apocyt *c* [7,14,15].

Nitrite and nitric oxide (NO), ubiquitous and highly toxic nitrogen oxides, can damage cells by directly reacting with the redox-active proteins, for instance with heme to form an

intermediate species with a ferrous-nitrogen dioxide character [16–19]. Nitrite has been traditionally used as a food preservative to inhibit the growth of undesirable bacteria for centuries, but its bacteriostatic effects are commonly attributed to NO [19,20]. However, recent studies have suggested that cellular targets of nitrite and NO are largely distinct, varying substantially even in the bacterial isolates in the same species [21–24]. Similarly, detoxification of nitrite and NO is carried out by different systems in bacteria [25]. While a large group of diverse enzymes catalyzes the transformation of nitrite to less-toxic nitrogen species, such as nitrate, ammonium, and dinitrogen gas, NO is primarily degraded by oxygen-dependent flavohemoglobin [26]. Moreover, proteins responsible for sensing nitrite and NO and mediating cellular responses to the resulting nitrosative stresses are also different, implying that bacterial cells treat these two nitrogen oxides distinctly in terms of physiology [25,26]. Thus, whether there is a common mechanism by which nitrite and NO influence bacterial physiology remains unknown.

*Shewanella oneidensis*, a Gram-negative  $\gamma$ -proteobacterium renowned for respiratory versatility, has served as a research model for extracellular electron transfer, a process that is largely based on a large repertoire of cyts *c* (up to 42) [5,27–29]. This unusually high cyt *c* content confers *S. oneidensis* cells (colony and cell pellet) a red-brown color, and given that the color intensity correlates well with the abundance of cyt *c*, it can be exploited to conveniently identify factors affecting the cyt *c* content [6,23,24,30,31]. More importantly, with this bacterium as a research model, we have demonstrated that cyts *c* constitute a defense frontline protecting metabolic enzymes from NO damage, whereas the primary targets of nitrite for oxygen respiration are heme-copper oxidase (HCO), including cyt *aa*<sub>3</sub> as in *Bacillus subtilis*, cyt *bo*<sub>3</sub> as in *E. coli*, and cyt *cbb*<sub>3</sub> as in *S. oneidensis* and *Pseudomonas aeruginosa* [23–25,32,33].

During our investigation, we noted that nitrite down-regulates the overall cyt *c* content, especially when fumarate is used as the electron acceptor (EA) to support growth [34]. This effect involves the cyclic adenosine monophosphate-catabolite repression protein (cAMP-Crp) transcriptional regulatory system, which mediates the transcription of a large number of genes encoding proteins involved in respiration, including many cyts *c* [32,34–36]. In this study, we first substantiate that the reduction in cAMP levels caused by nitrite or NO is not fully responsible for the decrease in the cyt *c* content in *S. oneidensis*. We then show that, although heme is implicated, its biosynthesis and cellular levels are not significantly affected by both of the nitrogen oxides. Further investigations reveal that nitrite and NO interfere with heme transport by compromising CcmE, leading to impaired cyt *c* biosynthesis.

## 2. Results

### 2.1. Nitrite and NO Down-Regulate cyt *c* Content of *S. oneidensis*

We found by chance that nitrite significantly reduces overall cyt *c* abundance in *S. oneidensis* wild-type (WT) cells grown on various EAs, fumarate in particular, as the cell pellets became evidently paler when nitrite was present [34] (Figure 1A,B). Given that nitrite shares similar biochemical properties with NO [19,26,37], we tested whether NO is also able to down-regulate the cyt *c* content in *S. oneidensis*. Indeed, a significant reduction in cyt *c* abundance was observed in cells grown in the presence of NO-releasing agent, NOC-18 (DETA-NONOate,  $t_{1/2} \approx 20$  h), at proper levels (Figure 1B and Figure S1). When NO scavenger carboxy-PTIO at 0.1 mM was added, which was able to quench the NO signal from NOC-18 to levels below the measurable limit, the cyt *c* content was not significantly altered (Figure 1B), validating the association of NO with the cyt *c* content. The application of carboxy-PTIO failed to prevent the cyt *c* content reduction in cells grown with nitrite (Figure 1B), eliminating the possibility that the observed effect of nitrite on the cyt *c* content is via NO. These data suggest that both nitrite and NO, independently of each other, are able to down-regulate the cyt *c* content in *S. oneidensis*.

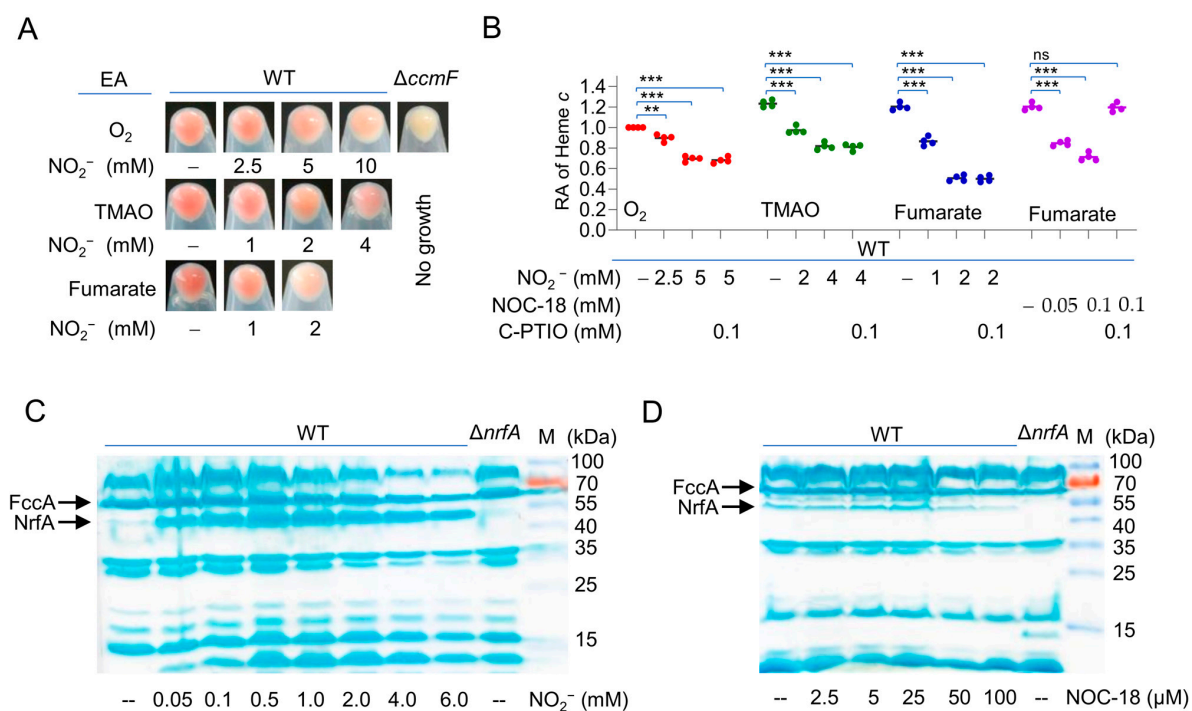


**Figure 1.** Nitrite and NO down-regulate cyt *c* content of *S. oneidensis*. **(A)** The cell color phenotypes. Shown are cell pellets of indicated strains grown on one of the EAs, O<sub>2</sub>, TMAO, and fumarate, to the early stationary phase. Strains include the wild-type (WT) and *cyt-c*-deficient  $\Delta CcmF$ . **(B)** Heme *c* levels. Samples prepared as in **(A)** were lysed for quantification of heme *c*. NOC-18 and C-PTIO were used as the NO producer and scavenger, respectively. The data were first adjusted to the protein levels of the samples, and then, the averaged heme *c* levels of the mutants were normalized to that in the WT, which was set to 1, giving the relative abundance (RA). Asterisks indicate statistically significant difference of the values compared ( $n = 4$ ; ns, not significant; \*\*,  $p < 0.01$ ; \*\*\*,  $p < 0.001$ ). **(C,D)** Heme staining. Samples prepared the same as for the quantification of heme *c* were processed; the protein contents were quantified, and equal amounts of the proteins were separated in SDS-PAGE, then subjected to heme staining. M, molecular weight marker. FccA and NrfA are indicated by arrows. All experiments were performed three times, and representatives as in **(A,C,D)** are presented.

In order to unravel the underlying mechanism for the effect, we compared cyt *c* profiles in the extracts of *S. oneidensis* WT cells grown on fumarate without or with nitrite at varying concentrations by heme staining. Nitrite at concentrations no less than 2 mM showed a negative effect on the abundance of all cyts *c*, including fumarate reductase FccA and nitrite reductase NrfA, verified by gene-deletion mutants and mass spectrometry (MS) analysis previously [6,38,39] (Figure 1C). Similar results were obtained from NO, whose effects on the cyt *c* content became evident when it was generated from NOC-18 at 50  $\mu$ M or higher (Figure 1D). It should be noted that the effects of nitrite and NO on the cyt *c* content can only be assessed non-quantitatively as the minimal inhibitory concentrations of these two nitrogen oxides on growth differ substantially [23,24]. Despite this, the reduced overall amounts of cyts *c* in the presence of either nitrite or NO at high concentrations were consistent with the data of heme *c* quantification (Figure 1B). These results conclude that both nitrite and NO impact the cyt *c* content, likely through a similar mechanism, and we therefore use nitrite/NO to simplify the description hereafter.

## 2.2. Nitrite/NO Compromise the cyt *c* Content in Growing Cells Only

It is fully established that hemoproteins are the primary targets of nitrite/NO by in vitro analyses [1,17,23,26,37]. We therefore moved on to test whether the reduction in the cyt *c* content caused by nitrite/NO is a result of cyt *c* damage and/or destruction. To this end, WT cells grown to the early stationary phase were collected and disrupted by

sonication, and the cell debris was treated with nitrite/NO at different concentrations for 5 h. Even with 10 mM nitrite or NOC-18, the cyt *c* content of the samples was not found to be significantly altered before and after the treatments (Figure 2A and Figure S2A), suggesting that nitrite/NO are unlikely able to release heme molecules from cyts *c*. To confirm this, bovine heart cyt *c* acquired commercially was incubated for 5 h with nitrite and NOC-18 at concentrations up to 120 mM and 10 mM, respectively. It was immediately evident that NOC-18 at 10 mM, but not nitrite at 120 mM, showed a visible influence on the color of the bovine heart cyt *c* solution, which became more pinkish (Figure S2B). Treated cyt *c* was then examined by SDS-PAGE/heme staining and spectroscopic measurements. As shown in Figure 2B, the migration of this protein was found unaffected by nitrite at all concentrations under test. However, although the treatment with NOC-18 at concentrations 5 mM or less was not able to elicit a detectable difference in bovine heart cyt *c*, a portion of the protein appeared to be modified with 10 mM NOC-18, probably due to the formation of the nitrosyl complex [17]. This was validated by the UV–visible absorption analysis. The spectrum of cyt *c* can be characterized by absorption of  $\gamma$ - (405 nm) and  $\alpha$ - (550 nm) Soret bands. Solutions of this cyt *c* in ferric form exhibited a Soret absorption at 405 nm with an unresolved  $\alpha$  band at 550 nm (Figure 2C). The addition of 10 mM NOC-18 generated a Soret absorption at 415 nm and evidently a band at 550 nm, which is typical for ferrous cyt *c*. The shift in Soret absorption was from 405 to 415 nm, which is the signature of the Fe(III)-nitrite complex [40,41]. In contrast, the cyt *c* treated by up to 20 mM nitrite was not different in the UV–visible absorption spectra from the untreated control (2D).

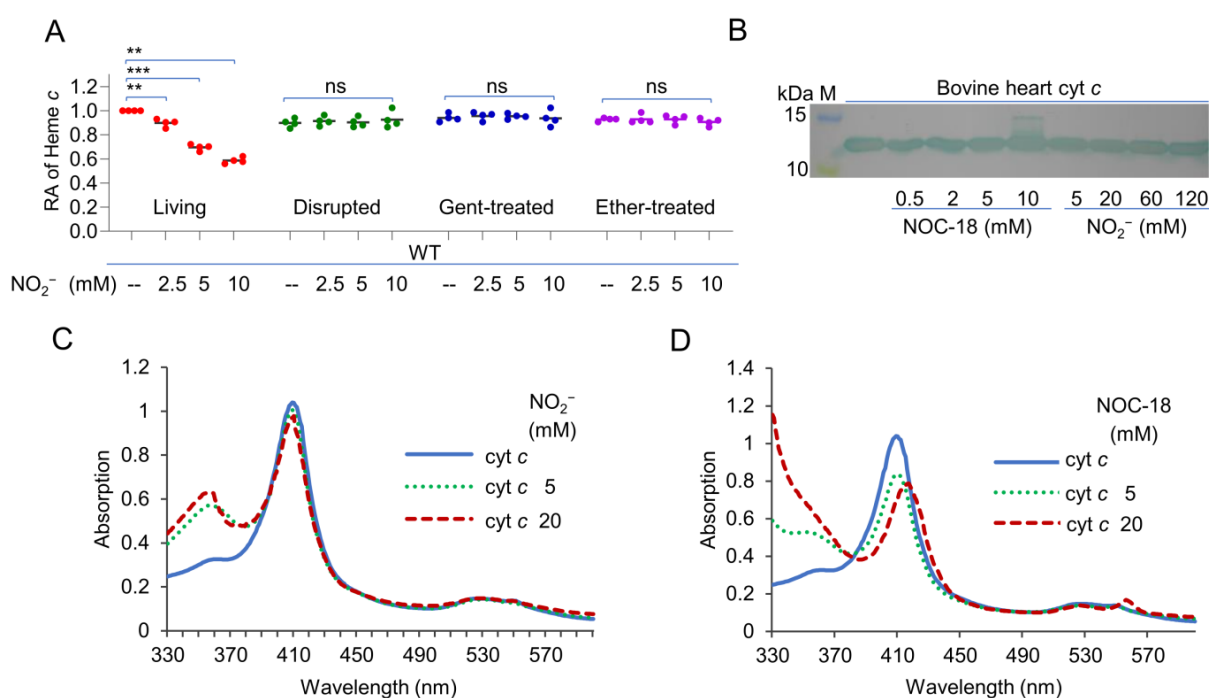


**Figure 2.** Nitrite and NO compromise the cyt *c* content in growing cells only. (A) Heme *c* levels. Cells at the early stationary phase were collected and processed by sonication or killed without destroying the cell morphology by treated with gentamycin or ether. All these samples were incubated with nitrite at varying concentrations for 5 h. Quantification of heme *c* was performed, and the data were processed as described in Figure 1b. Asterisks indicate statistically significant difference of the values compared ( $n = 4$ ; ns, not significant; \*\*,  $p < 0.01$ ; \*\*\*,  $p < 0.001$ ). (B) Heme staining. Bovine heart cyt *c* (2  $\mu\text{M}$ ) was incubated with nitrite and NO at the indicated concentrations for 5 h and then was examined by SDS-PAGE/heme staining. M, molecular weight marker. (C,D) UV–visible spectra of 5  $\mu\text{M}$  cyt *c* solutions. Shown are untreated and treated with nitrite C or NOC-18 (D) at indicated concentrations for 5 h. In (B–D), experiments were performed three times, and a representative as in (B) and the averaged as in (C,D) are presented.

Despite the observed modification of cyt *c* by NO of high concentrations, it is unlikely the reason for the substantial reduction in the cyt *c* content in living cells. To provide evidence, we assessed whether the effect of nitrite/NO can only be observed from viable cells. Cells prepared as above were subjected to either gentamycin (Gent) sulfate or ether treatment. Although both Gent- and ether-treated cells are non-viable, but intact, the latter differ from the former in that they can still carry out many biological processes, such as DNA synthesis and peptidoglycan synthesis, provided that the required substrates are supplemented [42,43]. Despite this difference, after incubation with 10 mM nitrite/NO for 5 h, the cyt *c* contents in samples before and after each of the treatments were not significantly different (Figure 2A and Figure S2A), suggesting that the impact of nitrite/NO is not effective with respect to these non-viable cells. Based on all of these data, we concluded that, despite their inhibitory effects on cyt *c* activity, nitrite/NO compromise the overall cyt *c* content only in viable cells because they are unable to break the covalent bond between heme molecules and the peptide at the physiologically relevant concentrations.

### 2.3. cAMP-CRP Is Not Exclusively Responsible for the Nitrite-/NO-Mediated Reduction in the cyt *c* Content

As nitrite/NO reduce the cyt *c* content not by directly disrupting cyts *c* per se, we reasoned that these molecules may down-regulate the expression of a significant share, if not all, of the genes for cyts *c*. In *S. oneidensis*, it is well established that the compromised activity of cAMP-Crp, which is the master regulatory system for respiration and directly controls transcription of a large portion of cyt *c* genes, results in a reduced cyt *c* content [32–35,44–46]. More importantly, nitrite has been implicated in down-regulating intracellular concentrations of cAMP, leading to lowered activity of cAMP-Crp [34]. However, whether the reduction in the cAMP levels exclusively accounts for the reduced content of cyts *c* caused by nitrite is unknown.

We reasoned that this can be assessed with Crp mutants that no longer require cAMP for activity. In *E. coli*, a Crp mutant, *EcCrp*<sup>T128L-S129I</sup>, showed a cAMP-independent DNA binding affinity comparable with that of cAMP-bound wild-type *EcCrp* [47]. In accord with the high sequence similarity (BLASTp E-value, 5e-139) between *E. coli* and *S. oneidensis* Crp proteins, *EcCrp* has been shown to be functional in *S. oneidensis* [35]. Despite this, the specific regulatory activity of *EcCrp* in *S. oneidensis* was determined with well-characterized CRP-dependent promoters, *P*<sub>CC(-41.5)</sub> and *P*<sub>cyd</sub>. While *P*<sub>CC(-41.5)</sub> is a semisynthetic derivative of the *melR* promoter of *E. coli*, *P*<sub>cyd</sub> directs transcription of the *cyd* operon encoding cyt *bd* oxidase in *S. oneidensis* [32,48]. DNA fragments for all Crp variants were placed under IPTG-inducible promoter *P*<sub>tac</sub> within expression vector pHGE-Ptac used repeatedly in *S. oneidensis* [49]. As expected, *EcCrp* and *EcCrp*<sup>T128L-S129I</sup>, the same as *SoCrp*, could activate the expression of both promoters in the  $\Delta$ *crp* strain in the presence of 0.1 mM IPTG (Figure 3A). Such an activating effect was still observed with *EcCrp*<sup>T128L-S129I</sup> in the absence of cAMP ( $\Delta$ *crp* $\Delta$ *cya*, lacking all three genes for adenylate cyclases (ACs)), and in contrast, neither *P*<sub>CC(-41.5)</sub> nor *P*<sub>cyd</sub> were responsive to the induced expression of *EcCrp* and *SoCrp* with up to 0.5 mM IPTG (Figure S3). These data validate that *EcCrp*<sup>T128L-S129I</sup> could function in a cAMP-independent manner as a transcriptional activator in *S. oneidensis*.

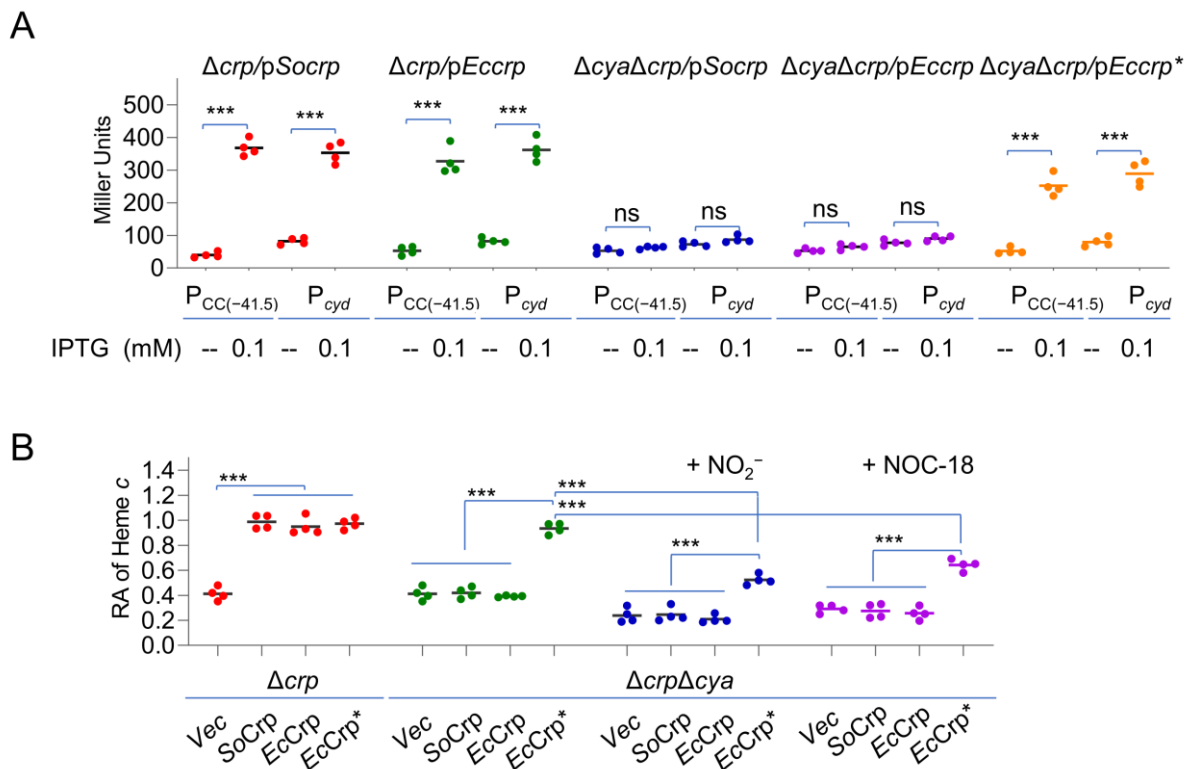


**Figure 3.** cAMP-CRP is not exclusively responsible for the nitrite-/NO-mediated reduction in the cyt *c* content. **(A)** *EcCrp*<sup>T128L-S129I</sup> (encoded by *Eccrp*<sup>\*</sup>) is independent of cAMP in *S. oneidensis*. Production of *SoCrp*, *EcCrp*, and *EcCrp*<sup>T128L-S129I</sup> was driven by the IPTG-inducible promoter in the *S. oneidensis* *crp* and *crp-cya* (missing all enzymes for cAMP synthesis) mutants.  $P_{CC(-41.5)}$  and  $P_{cyd}$  are promoters that are directly controlled by *EcCrp* and *SoCrp*, respectively. Promoter activity in cells grown to the early stationary phase was determined by LacZ reporters. **(B)** Heme *c* levels in the *S. oneidensis* *crp* and *crp-cya* mutants producing *SoCrp*, *EcCrp*, and *EcCrp*<sup>T128L-S129I</sup> with IPTG at 0.1 mM. Effects of 5 mM nitrite and 0.1 mM NOC-18 on *EcCrp*<sup>T128L-S129I</sup> were compared. Vec, empty vector. Asterisks indicate statistically significant difference of the values compared ( $n = 4$ ; ns, not significant; \*\*\*,  $p < 0.001$ ).

When grown on oxygen, both *crp* and *cya* mutants contained significantly decreased cyt *c* contents, approximately by 40% relative to the wild-type level (Figure 3B). The defect in the cyt *c* content of the  $\Delta crp$  strain can be fully corrected by the expression of *SoCrp*, *EcCrp*, or *EcCrp*<sup>T128L-S129I</sup> with 0.1 mM IPTG. However, *EcCrp*<sup>T128L-S129I</sup>, but not *EcCrp* or *SoCrp*, produced with IPTG 0.1 mM and above fully restored the cyt *c* content of  $\Delta crp\Delta cya$  to the wild-type level (Figure 3B). Despite this, nitrite/NO were still able to significantly reduce the cyt *c* content of  $\Delta crp\Delta cya$  expressing *EcCrp*<sup>T128L-S129I</sup> (Figure 3B). Based on this, we concluded that the nitrite-/NO-mediated reduction in the cyt *c* content in *S. oneidensis* could not be attributed to decreased cAMP levels exclusively.

#### 2.4. Increased Heme Levels Alleviate the Effect of Nitrite/NO on the cyt *c* Content

cyts *c* differ from other hemoproteins in that their heme *b* molecules are covalently attached to HBMs [2]. Given that heme is a substrate of cyt *c*, we hypothesized that the ligand may be a factor implicated in the reduced cyt *c* content caused by nitrite/NO. *S. oneidensis* possessing the common pathway for heme synthesis (Figure 4A), which entails nine reactions that convert glutamyl-tRNA to protoporphyrin IX [46,50]. HemaA (glutamyl-tRNA reductase) catalyzes the first dedicated, rate-limiting step in heme synthesis [51] (Figure 4A). To test whether nitrite/NO affect the synthesis of heme, we assessed the impacts of nitrite/NO on the expression of the *hemaA* gene, as well as two other *hem* genes and found that the impact was insignificant (Figure S4A). In line with this, we found that the nitrite/NO supplement did not significantly alter the heme levels in the cells

(Figure S4B). Nevertheless, we continued to examine whether increased heme production could counteract the effect of nitrite/NO on the *cyt c* content. As 5-ALA is used exclusively for heme production and its synthesis is a critical focal point for the regulation of heme biosynthesis [51], we first determined if exogenous 5-ALA influences the *cyt c* contents of *S. oneidensis* cells. In line with the previous observations [52], the addition of 50  $\mu$ M 5-ALA induced a noticeable increase in *cyt c* abundance, and a 35% increase was observed with 200  $\mu$ M ALA (Figure 4B). A similar effect of 5-ALA addition was observed in the presence of nitrite/NO despite the overall lowered *cyt c* levels.

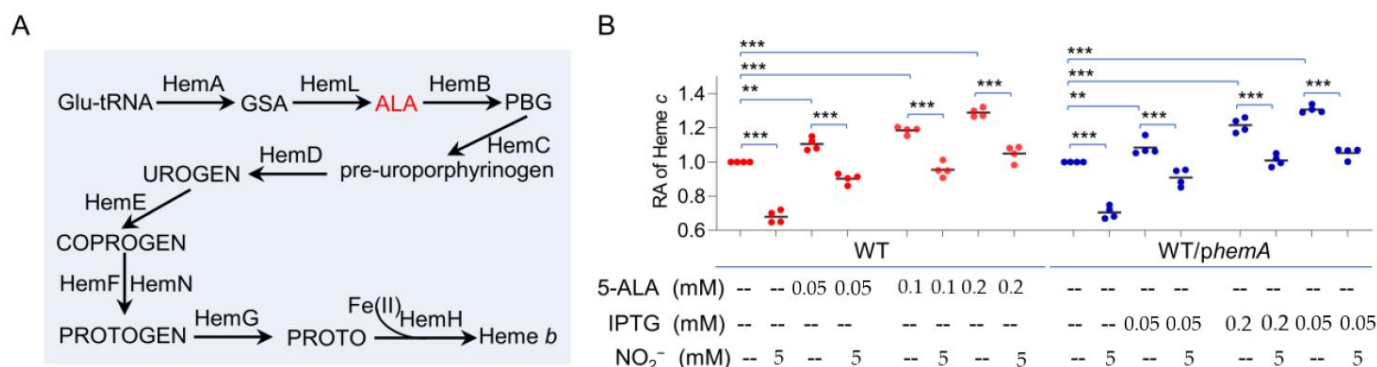


**Figure 4.** Heme antagonizes inhibitory effects of nitrite on the *cyt c* content. **(A).** Biosynthesis pathway of heme *b* in *S. oneidensis*. GSA, glutamate-1-semialdehyde; ALA, 5-aminolevulinic acid; PBG, porphobilinogen; UROGEN, uroporphyrinogen III; CORROGEN, coproporphyrinogen III; PROTOGEN, protoporphyrinogen IX; PROTO, protoporphyrin IX. **(B).** Heme *c* levels were quantified and are presented as relative abundance (RA). 5-ALA, the intermediate dictating the heme biosynthesis rate. Production of HemA was driven by the IPTG-inducible promoter in *S. oneidensis*. Asterisks indicate statistically significant difference of the values compared ( $n = 4$ ; ns, not significant; \*\*,  $p < 0.01$ ; \*\*\*,  $p < 0.001$ ).

The improving effect of elevated heme levels on the *cyt c* content was further assessed with manipulated *hemA* expression. In cells grown under normal conditions, the activity of the *hemA* promoter was not higher than that of  $P_{tac}$  with 0.05 mM IPTG [23,46]. As shown in Figure 4B, HemA overproduction with 0.2 mM IPTG was able to improve *cyt c* content by approximately 30%, but no further increase was observed with higher concentrations. Importantly, the effect of HemA in excess was also evident when 5.0 mM nitrite or 0.1 mM NOC-18 was present (Figure 4B and Figure S4C). These results suggest that heme may have a role in nitrite-mediated reduction in *cyt c* content.

### 2.5. Identification of *CcmE* as a Likely Target of Nitrite/NO on *cyt c* Production

To elucidate the involvement of heme in the effect of nitrite/NO on *cyt c* production, we turned to the CCM system. *S. oneidensis* possesses a highly conserved CCM system for *cyt c* biosynthesis, but its components are arranged into functional modules encoded by three operons, *ccmABCDE* (heme delivery), *ccmI*, and *CcmFGH* (heme-apocytochrome *c* ligation), in the *ccm* locus, in contrast to a single operon for the *ccm* genes present in most other  $\gamma$ -proteobacteria [4,6] (Figure S5A). After being synthesized in the cytoplasm, the apocytochromes *c* and heme *b* molecules are exported to the periplasmic compartment via the classical Sec protein secretion apparatus and by the CcmABCDE module, respectively, where the ligation between heme and HBM occurs [11,14] (Figure 5A). To test which functional module is implicated in nitrite-mediated reduction in *cyt c* content, we overexpressed each of them in WT cells. As shown in Figure 5B, in the presence of 5.0 mM nitrite, the lowered *cyt c* content could not be rescued by overproduction of either CcmFGH or CcmI. In contrast, overproduction of CcmABCDE was able to modestly improve *cyt c* production when nitrite was present, suggesting that heme delivery may be subject to nitrite inhibition. Further investigations showed that the overproduction of CcmE, but not CcmABCD was able to

improve the production of *cyt c* when nitrite was present, implying that nitrite may affect the physiological function of CcmE (Figure 5B).

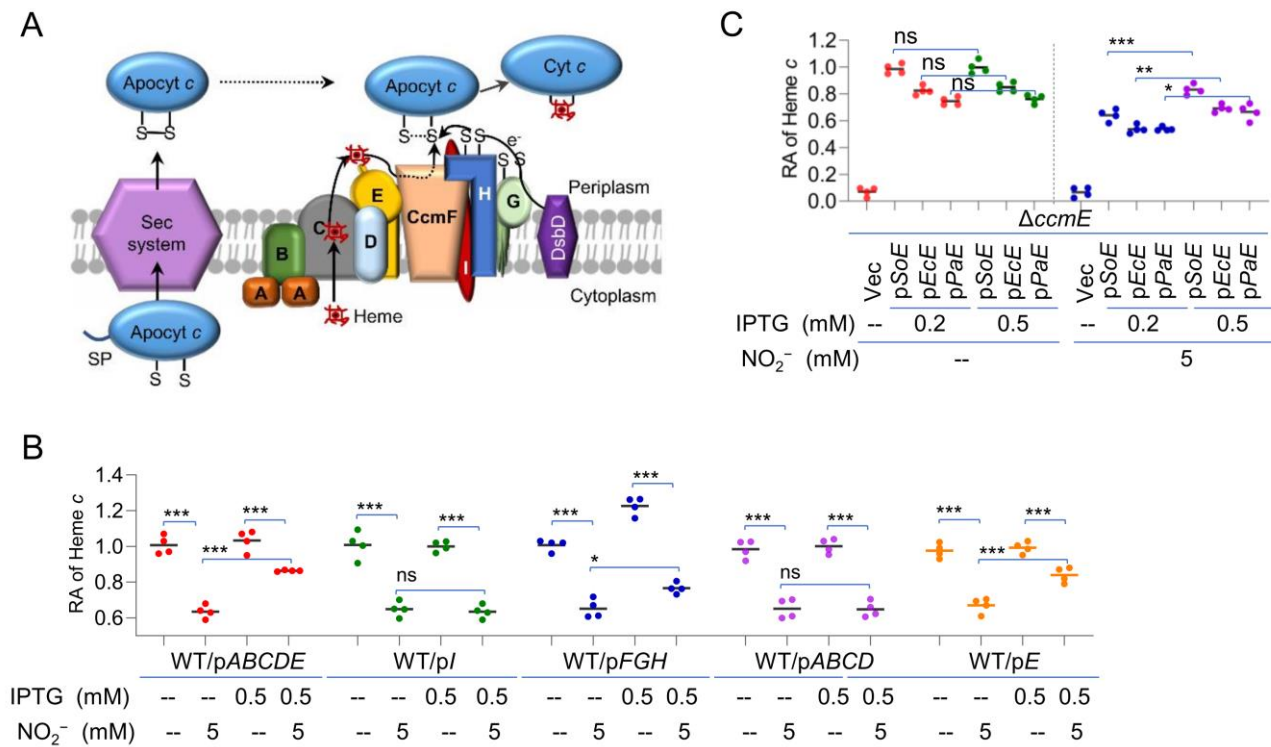


**Figure 5.** CcmE is a likely target of nitrite/NO in *cyt c* production. (A) A simplified model for *cyt c* biosynthesis in *S. oneidensis*. Both *apocyt c* and intracellular heme are transported to the periplasm, where heme attachment occurs. CcmABC transports heme across the membrane and delivers it to CcmE. CcmE then delivers heme to CcmF, which catalyzes heme attachment. (B) Heme *c* levels in WT overproducing Ccm components driven by the IPTG-inducible promoter without or with 5 mM nitrite. (C) Heme *c* levels in the *ccmE* mutant overproducing CcmE of *S. oneidensis* (SoE), *E. coli* (EcE), and *P. aeruginosa* (PaE) driven by the IPTG-inducible promoter without or with 5 mM nitrite. Asterisks indicate statistically significant difference of the values compared ( $n = 4$ ; ns, not significant; \*,  $p < 0.05$ ; \*\*,  $p < 0.01$ ; \*\*\*,  $p < 0.001$ ).

For confirmation, we constructed a *ccmE* mutant and monitored how the *cyt c* content changed in response to CcmE produced at varying levels. The results revealed that the  $\Delta ccmE$  strain was indistinguishable from the  $\Delta ccmF$  strain and the WT when a copy of *ccmE* was expressed in trans with IPTG at 0.2 mM and above (Figure S5B). Clearly, CcmE is essential for *cyt c* maturation in *S. oneidensis*, but it would not enhance the overall *cyt c* content when overproduced alone (Figure 5B). However, in the presence of nitrite, the effect of overproduced CcmE became evident: it antagonized the inhibition of nitrite (Figure 5C). Similar results were observed with NO (Figure S5C). Moreover, we tested whether nitrite would impact the activity of CcmE proteins in general. When CcmE proteins of *E. coli* and *P. aeruginosa* were overexpressed in the  $\Delta ccmE$  strain, both were found to be able to counteract the effect of nitrite on the *cyt c* biosynthesis to some extent, albeit not so effective as the *S. oneidensis* counterpart (Figure 5C and Figure S5D). Altogether, these data suggest that the reduced production of the *cyt c* content in the presence of nitrite/NO is, at least in part, due to the compromised CcmE activity.

### 2.6. Nitrite/NO Impair CcmE Activity through a Complex Mechanism

Among all System I components, CcmE is characterized by a unique feature in which it binds heme by way of a single covalent bond to a histidine [8]. As this covalent linkage



### 3. Discussion

Because of its bacteriostatic effect, nitrite has been used as a preservative in meat products for centuries. About 40 years ago, it was proposed that the bacteriostatic effect of nitrite is attributed to NO formation [20,53]. This appears reasonable, as in vitro studies show that nitrite and NO display similar, albeit not identical, biochemical properties, and therefore, the proteins susceptible to them are similar, mainly those containing redox-active centers such as heme, iron-sulfur clusters, mono-/di-nuclear iron, thiol, and so on [17,19,26,54]. In accord with this, most of the cellular targets identified in vivo to date are metabolic and respiratory enzymes depending on their redox-active centers for catalysis and/or oxi-reduction [55]. However, more recent investigations have revealed that key cellular targets of nitrite and NO in the bacterial species studied are largely different [22–25,55]. While the NO targets are primarily metabolic enzymes in the cytoplasm, nitrite specifically inhibits all types of HCOs, which are membrane-bound complexes exposed to the extracellular space [25]. This may be readily explained by the fact that NO diffuses into the cytoplasm freely, whereas nitrite is a charged and, therefore, membrane-impermeable molecule and has to rely on specific transporters to enter the cytoplasm in many bacteria [56,57]. It is therefore conceivable that the concentrations of nitrite on both sides of the membrane would make a difference.

Despite this, we continued in our endeavor to search for common targets of nitrite and NO in bacteria. In this study, by taking advantage of the high abundance of cyts *c* in *S. oneidensis* cells, we identified CcmE to be the one susceptible to both nitrite and NO. Although *S. oneidensis* is renowned for respiratory versatility, it has a limited capacity in dealing with nitrite [58]. Nitrite can only be transformed to ammonia without releasing any intermediate, and critically, this process occurs only in the absence of oxygen [59]. Similarly, the NO physiology of *S. oneidensis* is rather simple. This bacterium lacks not only an enzymatic source for NO generation, either bacterial nitric oxide synthase or denitrifying system, but also an efficient NO scavenger, such as flavohemoglobin [23,26,37].

One of the principal obstacles for this identification is that functional redundancy among factors regulating the cyt *c* content has limited the effectiveness of genetic analysis. To circumvent this, we managed to eliminate the influence of the cAMP-CRP regulatory system on the cyt *c* content, which functions as the master regulator in the respiration of *S. oneidensis* [35,45,46]. As nitrite compromises cAMP biosynthesis by a yet-unknown mechanism, it intertwines with the regulatory system in terms of the cyt *c* content [26,34]. By using a cAMP-independent Crp variant, we substantiated that nitrite/NO could cause a reduction in the cyt *c* content that is independent of cAMP-Crp. cyt *c* is formed by establishing a covalent linkage between two precursors, apocyt *c* and heme [2]. Given that cAMP-Crp impacts the cyt *c* content by directly mediating the transcription of a large number of cyt *c* genes, heme becomes a potential target whose homeostasis may be influenced by nitrite/NO. Our results support the notion that intracellular heme levels are not responsive to the addition of either nitrite or NO. This is not surprising as it has been well established that NO acts to block cellular heme insertion into a broad range of hemoproteins by either direct or indirect means, without affecting heme availability within the cells [60,61]. Nevertheless, heme at elevated concentrations was found to be able to relieve, at least partially, the suppression of nitrite/NO on the cyt *c* content. This antagonistic effect of heme on nitrite/NO inhibition has led to the identification of CcmE as a common target of nitrite and NO.

Although cyt *c* biosynthesis takes place in the periplasm, both precursors, apocyt *c* and heme, are generated in the cytoplasm [2]. Compared to the well-understood apocyt transmembrane transportation, heme delivery presents an interesting challenge for bacteria, which have to carry out multiple steps promptly, including intracellular heme traffic from the synthesized site to the CcmABC complex, heme transport through the inner membrane by CcmC, and heme transfer from CcmC to CcmE and, eventually, to CcmF [11,62–64]. Our data presented here suggest that the steps in which CcmE is involved are likely under the influence of nitrite/NO. When NO, presumably nitrite too, binds to heme, it typically decreases the strength of the axial bond formed between the heme iron and a

coordinating protein residue, weakening or even disrupting the bond [17,65]. Clearly, our data demonstrated that the covalent bonds within cyt *c* and CcmE, unlike those non-covalent ones within other hemoproteins, may not be disrupted by nitrite/NO at physiological relevant concentrations. However, the impacts of nitrite/NO on CcmE are apparent. The shifts in the UV–visible spectra of CcmE upon the treatment indicate that the protein is modified by both agents. The consequence of the modification is highly likely to form nitro coordination between nitrite and the protein, as revealed by a recent work that employed a variant of *alcaligenes xylooxidans* cyt *c*, which displays a remarkably increased heme affinity for nitrite [41].

In addition, we observed that the amount of CcmE detectable by heme staining reduces significantly. We do not yet know the underlying mechanism behind this. It is possible that the Fe(III)-nitrite complex is resistant to heme staining agents because of the loss of the redox activity. Meanwhile, it would be imprudent to exclude the possibility that these nitrogen oxides interfere with heme transfer from CcmC to CcmE. If this occurs, a portion of CcmE would exist in heme-free form, which has been shown to be inserted into the membrane and stable comparable to the heme-bound counterpart [13,66,67]. We are working to test this possibility.

The data presented also reveal an evident difference in the sensitivity to nitrite/NO between cyt *c* and CcmE. CcmE is substantially more susceptible to modification by nitrite/NO than cyt *c*, at least by four-fold. The enhanced susceptibility of CcmE to nitrite/NO explains why CcmE is inhibited by nitrite/NO in the presence of a large repertoire of cyts *c* in *S. oneidensis*. We envision that this modification impairs CcmE activity, thus lowering its heme delivery efficiency. While further investigations into this are underway, our current findings have highlighted a new mechanism by which nitrite/NO interfere with CcmE-mediated heme transfer to compromise cyt *c* maturation.

## 4. Materials and Methods

### 4.1. Bacterial Strains, Plasmids, and Culture Conditions

All bacterial strains and plasmids used in this study are listed in Table 1, and information about all of the primers used in this study is available upon request. All chemicals were obtained from Sigma (Shanghai, China), unless specifically noted. For genetic manipulation, *E. coli* and *S. oneidensis* were grown aerobically in lysogeny broth (LB, Difco, Detroit, MI, USA) at 37 and 30 °C. When appropriate, chemicals at the following concentrations were added to the growth medium: 2,6-diaminopimelic acid (DAP), 0.3 mM; kanamycin (Kan), 50 µg/mL; gentamycin (Gent), 15 µg/mL; catalase on plates, 2000 U/mL.

Growth of *S. oneidensis* strains under aerobic or anaerobic conditions was measured by recording the optical density of cultures at 600 nm (OD<sub>600</sub>). Defined medium MS containing 30 mM lactate as the electron donor and 20 mM TMAO or 20 mM fumarate as electron acceptor were used as previously described [68]. For aerobic growth, mid-log phase cultures were inoculated into fresh medium to an OD<sub>600</sub> of ~0.05 and shaken at 200 rpm at 30 °C. For anaerobic growth, mid-log phase aerobic cultures were pelleted by centrifugation, purged with nitrogen, and suspended in fresh media prepared anaerobically to an OD<sub>600</sub> of ~0.05.

### 4.2. Construction of in-Frame Deletion Strains

In-frame deletion strains for *S. oneidensis* were constructed according to the *att*-based Fusion PCR method, as described previously [5]. In brief, two fragments flanking the gene of interest were amplified by PCR, which were linked by the second round of PCR. The fusion fragments were integrated into plasmid pHGM01 by using Gateway BP clonase II enzyme mix (Invitrogen) according to the manufacturer's instruction. The resultant plasmid was transformed by electroporation into *E. coli* WM3064, and the verified ones were transferred to *S. oneidensis* strains by conjugation. Integration of the mutagenesis constructs into the chromosome was selected by resistance to gentamycin and confirmed by PCR. Verified trans-conjugants were grown in LB in the absence of NaCl and plated on

LB supplemented with 10% sucrose. Gentamycin-sensitive and sucrose-resistant colonies were screened by PCR for deletion of the target gene. Mutants were verified by sequencing the site for the intended mutation.

#### 4.3. Site-Directed Mutagenesis

Site-directed mutagenesis was performed to generate Crp proteins carrying point mutations using a QuikChange II XL site-directed mutagenesis kit (Stratagene) [69]. The *crp* gene within pHGEN-Ptac was subjected to modification, and the resulting products were digested by *DpnI* at 37 °C for 6 h and subsequently transformed into *E. coli* WM3064. The vectors carrying the intended mutations, which was verified by sequencing, were transferred into the relevant *S. oneidensis* strains by conjugation.

#### 4.4. Heme *c* Assays

Cultures of *S. oneidensis* strains grown in liquid medium to the early stationary phase were centrifuged, and the pellets were photographed. The *cyt c* abundance of strains was first estimated by the color intensity of the cell pellets. Subsequently, the pellets were suspended in PBS, adjusted to the same OD<sub>600</sub> values, and the cells from the same-volume aliquots were disrupted. All proteins were precipitated by trichloroacetic acid precipitation [70] and assayed for heme *c* levels with the QuantiChrom heme assay kit (BioAssay Systems) according to the manufacturer's instructions. If necessary, the values were normalized to the concentrations of the total proteins for each sample, which were determined by the bicinchoninic acid assay (Pierce Chemical) throughout this study.

#### 4.5. Controlled Gene Expression and Complementation of Mutants

Controlled gene expression was used in genetic complementation of mutants and assessment of the physiological effects of proteins at varying levels. The genes of interest were generated by PCR, cloned into plasmid pHGEN-Ptac under the control of Isopropyl β-D-1-thiogalactoside (IPTG)-inducible promoter Ptac, and the resultant vectors were transformed into *E. coli* WM3064 [71]. After verification by sequencing, the vectors were transferred into the relevant *S. oneidensis* strains via conjugation. Expression of the cloned genes was controlled by IPTG at varying concentrations.

#### 4.6. Preparation of Ether-Treated Bacterial Cells

*S. oneidensis* cells grown in LB under aerobic conditions to the early stationary phase (~0.8 of OD<sub>600</sub>) were harvested by centrifugation. From this sediment, ether-treated bacteria were prepared essentially as described by Mirelman et al. [72]. In brief, suspended cell samples of 5 mL (~0.8 of OD<sub>600</sub>) were mixed with ether under the conditions specified by Vosberg and Hoffmann-Berling [42]. After removal of the ether layer, the cells in the aqueous medium were sedimented (7000× *g*, 8 min), and the pellet was resuspended in basic medium at a concentration of approximately 10 mg of protein/mL (1010 cells/mL) and stored at −20 °C.

#### 4.7. Expression and Purification of Recombinant *CcmE*

The DNA fragment containing the sequences for the *ccmE* gene and for His<sub>6</sub>-tag was cloned into pHGEN-Ptac. *S. oneidensis* Δ*ccmE* carrying the resulting vector grown in LB to the mid-log phase was induced with 1 mM IPTG at 16 °C for 8 h and harvested by centrifugation. Cells were resuspended in Tris-HCl buffer (10 mM Tris-HCl, 150 mM NaCl, 1 mM EDTA, pH8.0), supplemented with 1 mM PMSF and 40 μg/mL DNase I (Roche). Cells were lysed by a high-pressure cell disruptor (JNBIO), cleared of cell debris by centrifugation at 20,000× *g* for 30 min at 4 °C, and followed by the separation of soluble and membrane fractions via high-speed ultracentrifugation at 160,000× *g* for 45 min at 4 °C. Membrane pellets were solubilized in Tris-HCl buffer with 1% n-dodecyl-β-D-maltopyranoside (Anatrace) and affinity purified by Beads IDA-Nickel (Solarbio). The subsequent purification steps

were performed according to the manufacturer's instructions. The purified proteins were analyzed by 12% SDS-PAGE, followed by staining with Coomassie Brilliant Blue R250.

#### 4.8. SDS-PAGE, Heme-Staining, and Western Blotting

Mid-log phase cells were harvested, washed with phosphate-buffered saline (PBS), resuspended in the same buffer, and sonicated. *cyt c* from bovine heart (Mol. Wt. 12,327) was acquired from Sigma-Aldrich Co. Protein concentrations of the cell lysates were determined by the bicinchoninic acid assay (Pierce Chemical). For heme staining, the cell lysates were separated by SDS-PAGE using 12% polyacrylamide gels and stained with 3,3',5,5'-tetramethylbenzidine (TMBZ), as described elsewhere [73]. His<sub>6</sub>-tagged recombinant CcmE was examined by Western blotting as described before [74]. Cell extracts for the detection of CcmE were subjected to electrophoresis on 10% SDS polyacrylamide gels (PAGE). Proteins were transferred to polyvinylidene difluoride (PVDF) membranes for 1 h at 60 V using a Criterion blotter (Bio-Rad). The blotting membrane was probed with antibodies against the His<sub>6</sub> tag (Sangon Biotech, Shanghai, China), followed by a 1:10,000 dilution of goat anti-rabbit immunoglobulin G-alkaline phosphatase conjugate. The alkaline phosphatase was detected using a chemiluminescence Western blotting kit (Roche Diagnostics) in accordance with the manufacturer's instructions. Images were visualized with Clinx Imaging System (Clinx, Shanghai, China).

#### 4.9. Spectroscopic Analysis

To explore the effects of nitrite and NO on *cyts c* and purified CcmE, UV-visible spectra were recorded on a Varioskan Flash (Thermo scientific, Shanghai, China). Protein was incubated with various concentrations of nitrite and NOC18 at room temperature for 20 min before the measurements were taken.

#### 4.10. $\beta$ -Galactosidase Activity Assay

The activity of the promoters of interest was assessed using a single-copy integrative *lacZ* reporter system as described previously [75]. The sequence in sufficient length (~400 bp) upstream of the gene of interest was amplified and inserted in front of the full-length *E. coli lacZ* gene in plasmid pHGEI01. The resulting plasmid was verified by sequencing, introduced into *E. coli* WM3064, and then, conjugated with relevant *S. oneidensis* strains. Once transferred into *S. oneidensis* strains, pHGEI01 containing the promoter of interest integrated into the chromosome, and the antibiotic marker was then removed by an established approach [32]. Cultures of the mid-exponential phase were collected by centrifugation, washed with PBS, and treated with lysis buffer (0.25 M Tris/HCl, 0.5% Triton X-100, pH 7.5). Extracts were collected by centrifugation and applied for the enzyme assay by adding o-nitrophenyl- $\beta$ -D-galactopyranoside (ONPG) (4 mg/mL). Changes in absorption over time were monitored at 420 nm with a Synergy 2 Pro200 Multi-Detection Microplate Reader (Tecan), and the results are presented as Miller units.

#### 4.11. Other Analyses

To estimate the relative abundance of the proteins in the gels, the intensities of the bands were quantified using ImageJ software [76]. Student's *t*-test was performed for pairwise comparisons. In the figures, the values are presented as the means  $\pm$  the standard deviation (SD).

**Table 1.** Strains and plasmids used in this study.

Strain or Plasmid	Description	Source/Reference
<i>E. coli</i> DH5 $\alpha$ WM3064	Host strain for plasmids Donor strain for conjugation; $\Delta$ dapA	Laboratory stock W. Metcalf, UIUC <sup>a</sup>
<i>S. oneidensis</i> MR-1	Wild type	ATCC 700550
HG0624	$\Delta$ crp derived from MR-1	[45]
HG0696	$\Delta$ ccmF derived from MR-1	[5]
HG0958	$\Delta$ nrfA derived from MR-1	[58]
HG1070	$\Delta$ ccmE derived from MR-1	This study
HG3901-0624	$\Delta$ cya $\Delta$ crp derived from MR-1	This study
Plasmids		
pHGM01	Ap <sup>r</sup> Gm <sup>r</sup> Cm <sup>r</sup> suicide vector	[5]
pHGEI01	Integrative lacZ reporter vector	[75]
pHGEN-Ptac	IPTG-inducible Ptac expression vector	[71]
pHGEI01-P <sub>hemA</sub>	For measuring P <sub>hemA</sub> activity	[46]
pHGEI01-P <sub>hemC</sub>	For measuring P <sub>hemC</sub> activity	[46]
pHGEI01-P <sub>hemH1</sub>	For measuring P <sub>hemH1</sub> activity	[77]
pHGEI01-P <sub>hemH2</sub>	For measuring P <sub>hemH2</sub> activity	[77]
pHGEI01-P <sub>CC(-41.5)</sub>	For measuring P <sub>CC(-41.5)</sub> activity	This study
pHGEI01-P <sub>cyd</sub>	For measuring P <sub>cyd</sub> activity	This study
pHGEN-Ptac-Socrp	For inducible production of <i>S. oneidensis</i> Crp	This study
pHGEN-Ptac-Eccrp	For inducible production of <i>E. coli</i> Crp	This study
pHGEN-Ptac-Eccrp*	For inducible production of cAMP-independent <i>E. coli</i> Crp	This study
pHGEN-Ptac-hemA	For inducible production of HemA	This study
pHGEN-Ptac-ccmI	For inducible production of CcmI	This study
pHGEN-Ptac-ccmABCDE	For inducible production of CcmABCDE	This study
pHGEN-Ptac-ccmABCD	For inducible production of CcmABCD	This study
pHGEN-Ptac-ccmFGH ccmABCD	For inducible production of CcmFGH	This study
pHGEN-Ptac-ccmE	For inducible production of <i>S. oneidensis</i> CcmE	This study
pHGEN-Ptac-EccmE	For inducible production of <i>E. coli</i> CcmE	This study
pHGEN-Ptac-PaccmE	For inducible production of <i>P. aeruginosa</i> CcmE	This study
pHGEN-Ptac-ccmE <sup>his</sup>	For inducible expression of His-tagged CcmE	This study

<sup>a</sup> UIUC, University of Illinois Urbana-Champaign.

**Supplementary Materials:** The following Supporting Information can be downloaded at: <https://www.mdpi.com/article/10.3390/ijms232213841/s1>.

**Author Contributions:** Conceptualization, H.G.; investigation, W.W., J.W. and X.F.; resources, H.G.; data curation, W.W. and H.G.; writing—original draft preparation, W.W.; writing—review and editing, H.G.; supervision, H.G.; funding acquisition, H.G. All authors have read and agreed to the published version of the manuscript.

**Funding:** This research was funded by National Natural Science Foundation of China (31930003, 41976087) and by National Key R&D Program of China (2018YFA0901300).

**Institutional Review Board Statement:** Not applicable.

**Informed Consent Statement:** Not applicable.

**Data Availability Statement:** Not applicable.

**Conflicts of Interest:** The authors declare no conflict of interest.

## References

- Alvarez-Paggi, D.; Hannibal, L.; Castro, M.A.; Oviedo-Rouco, S.; Demicheli, V.; Tórtora, V.; Tomasina, F.; Radi, R.; Murgida, D.H. Multifunctional cytochrome *c*: Learning new tricks from an old dog. *Chem. Rev.* **2017**, *117*, 13382–13460. [CrossRef] [PubMed]
- Kranz, R.G.; Richard-Fogal, C.; Taylor, J.-S.; Frawley, E.R. Cytochrome *c* biogenesis: Mechanisms for covalent modifications and trafficking of heme and for heme-iron redox control. *Microbiol. Mol. Biol. Rev.* **2009**, *73*, 510–528. [CrossRef] [PubMed]
- Verissimo, A.F.; Daldal, F. Cytochrome *c* biogenesis System I: An intricate process catalyzed by a maturase supercomplex. *Biochim. Biophys. Acta* **2014**, *1837*, 989–998. [CrossRef] [PubMed]
- Cianciotto, N.P.; Cornelis, P.; Baysse, C. Impact of the bacterial type I cytochrome *c* maturation system on different biological processes. *Mol. Microbiol.* **2005**, *56*, 1408–1415. [CrossRef]

5. Jin, M.; Jiang, Y.; Sun, L.; Yin, J.; Fu, H.; Wu, G.; Gao, H. Unique organizational and functional features of the cytochrome *c* maturation system in *Shewanella oneidensis*. *PLoS ONE* **2013**, *8*, e75610. [[CrossRef](#)] [[PubMed](#)]
6. Fu, H.; Jin, M.; Wan, F.; Gao, H. *Shewanella oneidensis* cytochrome *c* maturation component CcmI is essential for heme attachment at the non-canonical motif of nitrite reductase NrfA. *Mol. Microbiol.* **2015**, *95*, 410–425. [[CrossRef](#)] [[PubMed](#)]
7. Gao, M.; Nakajima An, D.; Parks, J.M.; Skolnick, J. AF2Complex predicts direct physical interactions in multimeric proteins with deep learning. *Nat. Commun.* **2022**, *13*, 1744. [[CrossRef](#)]
8. Schulz, H.; Hennecke, H.; Thöny-Meyer, L. Prototype of a heme chaperone essential for cytochrome *c* maturation. *Science* **1998**, *281*, 1197–1200. [[CrossRef](#)]
9. Feissner, R.E.; Richard-Fogal, C.L.; Frawley, E.R.; Kranz, R.G. ABC transporter-mediated release of a haem chaperone allows cytochrome *c* biogenesis. *Mol. Microbiol.* **2006**, *61*, 219–231. [[CrossRef](#)]
10. Richard-Fogal, C.L.; Frawley, E.R.; Bonner, E.R.; Zhu, H.; San Francisco, B.; Kranz, R.G. A conserved haem redox and trafficking pathway for cofactor attachment. *EMBO J.* **2009**, *28*, 2349–2359. [[CrossRef](#)]
11. Mendez, D.L.; Lowder, E.P.; Tillman, D.E.; Sutherland, M.C.; Collier, A.L.; Rau, M.J.; Fitzpatrick, J.A.J.; Kranz, R.G. Cryo-EM of CcsBA reveals the basis for cytochrome *c* biogenesis and heme transport. *Nat. Chem. Biol.* **2022**, *18*, 101–108. [[CrossRef](#)] [[PubMed](#)]
12. Lee, D.; Pervushin, K.; Bischof, D.; Braun, M.; Thöny-Meyer, L. Unusual heme–Histidine bond in the active site of a chaperone. *J. Am. Chem. Soc.* **2005**, *127*, 3716–3717. [[CrossRef](#)] [[PubMed](#)]
13. Harvat, E.M.; Redfield, C.; Stevens, J.M.; Ferguson, S.J. Probing the heme-binding site of the cytochrome *c* maturation protein CcmE. *Biochemistry* **2009**, *48*, 1820–1828. [[CrossRef](#)] [[PubMed](#)]
14. Stevens, J.M.; Mavridou, D.A.I.; Hamer, R.; Kritsiligkou, P.; Goddard, A.D.; Ferguson, S.J. Cytochrome *c* biogenesis System I. *FEBS J.* **2011**, *278*, 4170–4178. [[CrossRef](#)]
15. Brausemann, A.; Zhang, L.; Ilcu, L.; Einsle, O. Architecture of the membrane-bound cytochrome *c* heme lyase CcmF. *Nat. Chem. Biol.* **2021**, *17*, 800–805. [[CrossRef](#)]
16. Gladwin, M.T.; Grubina, R.; Doyle, M.P. The new chemical biology of nitrite reactions with hemoglobin: R-state catalysis, oxidative denitrosylation, and nitrite reductase/anhydrase. *Acc. Chem. Res.* **2008**, *42*, 157–167. [[CrossRef](#)]
17. Ford, P.C. Reactions of NO and nitrite with heme models and proteins. *Inorg. Chem.* **2010**, *49*, 6226–6239. [[CrossRef](#)]
18. Bowman, L.A.H.; McLean, S.; Poole, R.K.; Fukuto, J.M. The diversity of microbial responses to nitric oxide and agents of nitrosative stress: Close cousins but not identical twins. In *Advances in Microbial Physiology*; Robert, K.P., Ed.; Academic Press: Cambridge, MA, USA, 2011; Volume 59, pp. 135–219.
19. Maia, L.B.; Moura, J.J.G. How biology handles nitrite. *Chem. Rev.* **2014**, *114*, 5273–5357. [[CrossRef](#)]
20. Reddy, D.; Lancaster, J.; Cornforth, D. Nitrite inhibition of *Clostridium botulinum*: Electron spin resonance detection of iron-nitric oxide complexes. *Science* **1983**, *221*, 769–770. [[CrossRef](#)]
21. Hyduke, D.R.; Jarboe, L.R.; Tran, L.M.; Chou, K.J.Y.; Liao, J.C. Integrated network analysis identifies nitric oxide response networks and dihydroxyacid dehydratase as a crucial target in *Escherichia coli*. *Proc. Natl. Acad. Sci. USA* **2007**, *104*, 8484–8489. [[CrossRef](#)]
22. Richardson, A.R.; Payne, E.C.; Younger, N.; Karlinsey, J.E.; Thomas, V.C.; Becker, L.A.; Navarre, W.W.; Castor, M.E.; Libby, S.J.; Fang, F.C. Multiple targets of nitric oxide in the tricarboxylic acid cycle of *Salmonella enterica* Serovar Typhimurium. *Cell Host Microbe* **2011**, *10*, 33–43. [[CrossRef](#)]
23. Meng, Q.; Yin, J.; Jin, M.; Gao, H. Distinct nitrite and nitric oxide physiologies in *Escherichia coli* and *Shewanella oneidensis*. *Appl. Environ. Microbiol.* **2018**, *84*, e00559-18. [[CrossRef](#)]
24. Meng, Q.; Sun, Y.; Gao, H. Cytochromes *c* constitute a layer of protection against nitric oxide but not nitrite. *Appl. Environ. Microbiol.* **2018**, *84*, e01255-18. [[CrossRef](#)] [[PubMed](#)]
25. Guo, K.; Gao, H. Physiological roles of nitrite and nitric oxide in bacteria: Similar consequences from distinct cell targets, protection, and Sensing Systems. *Adv. Biol.* **2021**, *5*, 2100773. [[CrossRef](#)] [[PubMed](#)]
26. Zhang, Y.; Guo, K.; Meng, Q.; Gao, H. Nitrite modulates aminoglycoside tolerance by inhibiting cytochrome heme-copper oxidase in bacteria. *Commun. Biol.* **2020**, *3*, 269. [[CrossRef](#)]
27. Fredrickson, J.K.; Romine, M.F.; Beliaev, A.S.; Auchtung, J.M.; Driscoll, M.E.; Gardner, T.S.; Nealson, K.H.; Osterman, A.L.; Grigoriy, P.; Reed, J.L. Towards environmental systems biology of *Shewanella*. *Nat. Rev. Microbiol.* **2008**, *6*, 592–603. [[CrossRef](#)]
28. Meyer, T.E.; Tsapin, A.I.; Vandenbergh, I.; De Smet, L.; Frishman, D.; Nealson, K.H.; Cusanovich, M.A.; Van Beeumen, J.J. Identification of 42 possible cytochrome *c* genes in the *Shewanella oneidensis* genome and characterization of six soluble cytochromes. *OMICS J. Integr. Biol.* **2004**, *8*, 57–77. [[CrossRef](#)]
29. Gao, H.; Barua, S.; Liang, Y.; Wu, L.; Dong, Y.; Reed, S.; Chen, J.; Culley, D.; Kennedy, D.; Yang, Y.; et al. Impacts of *Shewanella oneidensis* *c*-type cytochromes on aerobic and anaerobic respiration. *Microb. Biotechnol.* **2010**, *3*, 455–466. [[CrossRef](#)]
30. Guo, K.; Wang, W.; Wang, H.; Lu, Z.; Gao, H. Complex oxidation of apocytochromes *c* during bacterial cytochrome *c* maturation. *Appl. Environ. Microbiol.* **2019**, *85*, e01989-19. [[CrossRef](#)] [[PubMed](#)]
31. Feng, X.; Sun, W.; Kong, L.; Gao, H. Distinct roles of *Shewanella oneidensis* thioredoxin in regulation of cellular responses to hydrogen and organic peroxides. *Appl. Environ. Microbiol.* **2019**, *85*, e01700-19. [[CrossRef](#)]
32. Fu, H.; Chen, H.; Wang, J.; Zhou, G.; Zhang, H.; Zhang, L.; Gao, H. Crp-dependent cytochrome *bd* oxidase confers nitrite resistance to *Shewanella oneidensis*. *Environ. Microbiol.* **2013**, *15*, 2198–2212. [[CrossRef](#)] [[PubMed](#)]

33. Zhou, G.; Yin, J.; Chen, H.; Hua, Y.; Sun, L.; Gao, H. Combined effect of loss of the *caa3* oxidase and Crp regulation drives *Shewanella* to thrive in redox-stratified environments. *ISME J.* **2013**, *7*, 1752–1763. [[CrossRef](#)] [[PubMed](#)]
34. Jin, M.; Fu, H.; Yin, J.; Yuan, J.; Gao, H. Molecular underpinnings of nitrite effect on CymA-dependent respiration in *Shewanella oneidensis*. *Front. Microbiol.* **2016**, *7*, 1154. [[CrossRef](#)]
35. Saffarini, D.A.; Schultz, R.; Beliaev, A. Involvement of cyclic AMP (cAMP) and cAMP receptor protein in anaerobic respiration of *Shewanella oneidensis*. *J. Bacteriol.* **2003**, *185*, 3668–3671. [[CrossRef](#)]
36. Jin, M.; Zhang, Q.; Sun, Y.; Gao, H. NapB in excess inhibits growth of *Shewanella oneidensis* by dissipating electrons of the quinol pool. *Sci. Rep.* **2016**, *6*, 37456. [[CrossRef](#)] [[PubMed](#)]
37. Chen, J.; Xie, P.; Huang, Y.; Gao, H. Complex interplay of heme-copper oxidases with nitrite and nitric oxide. *Int. J. Mol. Sci.* **2022**, *23*, 979. [[CrossRef](#)] [[PubMed](#)]
38. Schuetz, B.; Schickelberger, M.; Kuermann, J.; Spormann, A.M.; Gescher, J. Periplasmic electron transfer via the *c*-type cytochromes MtrA and FccA of MR-1. *Appl. Environ. Microbiol.* **2009**, *75*, 7789–7796. [[CrossRef](#)]
39. Dong, Y.; Wang, J.; Fu, H.; Zhou, G.; Shi, M.; Gao, H. A Crp-dependent two-component system regulates nitrate and nitrite respiration in *Shewanella oneidensis*. *PLoS ONE* **2012**, *7*, e51643. [[CrossRef](#)]
40. Korobko, V.M.; Melnikova, N.B.; Pantelev, D.A.; Martusevich, A.K.; Peretyagin, S.P. The study of the complexes of nitromedicine with cytochrome *c* and NO-containing aqueous dosage form in the wound treatment of rats. *Nitric Oxide* **2014**, *42*, 62–69. [[CrossRef](#)]
41. Nilsson, Z.N.; Mandella, B.L.; Sen, K.; Kekilli, D.; Hough, M.A.; Moënne-Loccoz, P.; Strange, R.W.; Andrew, C.R. Distinguishing nitro vs. nitrito coordination in cytochrome *c'* using vibrational spectroscopy and density functional theory. *Inorg. Chem.* **2017**, *56*, 13205–13213. [[CrossRef](#)]
42. Vosberg, H.-P.; Hoffmann-Berling, H. DNA synthesis in nucleotide-permeable *Escherichia coli* cells: I. Preparation and properties of ether-treated cells. *J. Mol. Biol.* **1971**, *58*, 739–753. [[CrossRef](#)]
43. Paradis-Bleau, C.; Markovski, M.; Uehara, T.; Lupoli, T.J.; Walker, S.; Kahne, D.E.; Bernhardt, T.G. Lipoprotein cofactors located in the outer membrane activate bacterial cell wall polymerases. *Cell* **2010**, *143*, 1110–1120. [[CrossRef](#)] [[PubMed](#)]
44. Charania, M.A.; Brockman, K.L.; Zhang, Y.; Banerjee, A.; Pinchuk, G.E.; Fredrickson, J.K.; Beliaev, A.S.; Saffarini, D.A. Involvement of a membrane-bound class III adenylate cyclase in regulation of anaerobic respiration in *Shewanella oneidensis* MR-1. *J. Bacteriol.* **2009**, *191*, 4298–4306. [[CrossRef](#)]
45. Gao, H.; Wang, X.; Yang, Z.; Chen, J.; Liang, Y.; Chen, H.; Palzkill, T.; Zhou, J. Physiological roles of ArcA, Crp, and EtrA and their interactive control on aerobic and anaerobic respiration in *Shewanella oneidensis*. *PLoS ONE* **2010**, *5*, e15295. [[CrossRef](#)]
46. Yin, J.; Meng, Q.; Fu, H.; Gao, H. Reduced expression of cytochrome oxidases largely explains cAMP inhibition of aerobic growth in *Shewanella oneidensis*. *Sci. Rep.* **2016**, *6*, 24449. [[CrossRef](#)] [[PubMed](#)]
47. Youn, H.; Kerby, R.L.; Conrad, M.; Roberts, G.P. Study of highly constitutively active mutants suggests how cAMP activates cAMP receptor protein\*. *J. Biol. Chem.* **2006**, *281*, 1119–1127. [[CrossRef](#)] [[PubMed](#)]
48. Savery, N.J.; Lloyd, G.S.; Kainz, M.; Gaal, T.; Ross, W.; Ebright, R.H.; Gourse, R.L.; Busby, S.J.W. Transcription activation at class II CRP-dependent promoters: Identification of determinants in the C-terminal domain of the RNA polymerase  $\alpha$  subunit. *EMBO J.* **1998**, *17*, 3439–3447. [[CrossRef](#)]
49. Luo, Q.; Dong, Y.; Chen, H.; Gao, H. Mislocalization of rieske Protein PetA predominantly accounts for the aerobic growth defect of tat mutants in *Shewanella oneidensis*. *PLoS ONE* **2013**, *8*, e62064. [[CrossRef](#)]
50. Layer, G. Heme biosynthesis in prokaryotes. *Biochim. Biophys. Acta Mol. Cell. Res.* **2021**, *1868*, 118861. [[CrossRef](#)]
51. Dailey, H.A.; Dailey, T.A.; Gerdes, S.; Jahn, D.; Jahn, M.; O'Brian, M.R.; Warren, M.J. Prokaryotic heme biosynthesis: Multiple pathways to a common essential product. *Microbiol. Mol. Biol. Rev.* **2017**, *81*, e00048-16. [[CrossRef](#)]
52. Brennan, C.M.; Mazzucca, N.Q.; Mezoian, T.; Hunt, T.M.; Keane, M.L.; Leonard, J.N.; Scola, S.E.; Beer, E.N.; Perdue, S.; Pellock, B.J. Reduced heme levels underlie the exponential growth defect of the *Shewanella oneidensis* *hfq* mutant. *PLoS ONE* **2014**, *9*, e109879. [[CrossRef](#)]
53. Yang, T. Mechanism of nitrite inhibition of cellular respiration in *Pseudomonas aeruginosa*. *Curr. Microbiol.* **1985**, *12*, 35–39. [[CrossRef](#)]
54. Tonzetich, Z.J.; McQuade, L.E.; Lippard, S.J. Detecting and understanding the roles of nitric oxide in biology. *Inorg. Chem.* **2010**, *49*, 6338–6348. [[CrossRef](#)] [[PubMed](#)]
55. Stern, A.M.; Zhu, J. Chapter Five—An introduction to nitric oxide sensing and response in bacteria. In *Advances in Applied Microbiology*; Sima, S., Geoffrey, M.G., Eds.; Academic Press: Cambridge, MA, USA, 2014; Volume 87, pp. 187–220.
56. Samouilov, A.; Woldman, Y.Y.; Zweier, J.; Khramtsov, V. Magnetic resonance study of the transmembrane nitrite diffusion. *Nitric Oxide* **2007**, *16*, 362–370. [[CrossRef](#)] [[PubMed](#)]
57. Lü, W.; Du, J.; Schwarzer, N.J.; Wacker, T.; Andrade, S.L.; Einsle, O. The formate/nitrite transporter family of anion channels. *Biol. Chem.* **2013**, *394*, 715–727. [[CrossRef](#)]
58. Gao, H.; Yang, Z.K.; Barua, S.; Reed, S.B.; Romine, M.F.; Nealson, K.H.; Fredrickson, J.K.; Tiedje, J.M.; Zhou, J. Reduction of nitrate in *Shewanella oneidensis* depends on atypical NAP and NRF systems with NapB as a preferred electron transport protein from CymA to NapA. *ISME J.* **2009**, *3*, 966–976. [[CrossRef](#)]
59. Zhang, H.; Fu, H.; Wang, J.; Sun, L.; Jiang, Y.; Zhang, L.; Gao, H. Impacts of nitrate and nitrite on physiology of *Shewanella oneidensis*. *PLoS ONE* **2013**, *8*, e62629. [[CrossRef](#)]

60. Albakri, Q.A.; Stuehr, D.J. Intracellular assembly of inducible NO synthase is limited by nitric oxide-mediated changes in heme insertion and availability. *J. Biol. Chem.* **1996**, *271*, 5414–5421. [[CrossRef](#)]
61. Waheed, S.M.; Ghosh, A.; Chakravarti, R.; Biswas, A.; Haque, M.M.; Panda, K.; Stuehr, D.J. Nitric oxide blocks cellular heme insertion into a broad range of heme proteins. *Free Radic. Biol. Med.* **2010**, *48*, 1548–1558. [[CrossRef](#)]
62. Richard-Fogal, C.; Kranz, R.G. The CcmC:heme:CcmE complex in heme trafficking and cytochrome *c* biosynthesis. *J. Mol. Biol.* **2010**, *401*, 350–362. [[CrossRef](#)]
63. Shevket, S.H.; Gonzalez, D.; Cartwright, J.L.; Kleanthous, C.; Ferguson, S.J.; Redfield, C.; Mavridou, D.A.I. The CcmC–CcmE interaction during cytochrome *c* maturation by System I is driven by protein–protein and not protein–heme contacts. *J. Biol. Chem.* **2018**, *293*, 16778–16790. [[CrossRef](#)] [[PubMed](#)]
64. Gallio, A.E.; Fung, S.S.P.; Cammack-Najera, A.; Hudson, A.J.; Raven, E.L. Understanding the logistics for the distribution of heme in cells. *JACS Au* **2021**, *1*, 1541–1555. [[CrossRef](#)] [[PubMed](#)]
65. Cooper, C.E. Nitric oxide and iron proteins. *Biochim. Biophys. Acta* **1999**, *1411*, 290–309. [[CrossRef](#)]
66. Daltrop, O.; Allen, J.W.A.; Willis, A.C.; Ferguson, S.J. In vitro formation of a *c*-type cytochrome. *Proc. Natl. Acad. Sci. USA* **2002**, *99*, 7872–7876. [[CrossRef](#)] [[PubMed](#)]
67. Uchida, T.; Stevens, J.M.; Daltrop, O.; Harvat, E.M.; Hong, L.; Ferguson, S.J.; Kitagawa, T. The interaction of covalently bound heme with the cytochrome *c* maturation protein CcmE. *J. Biol. Chem.* **2004**, *279*, 51981–51988. [[CrossRef](#)] [[PubMed](#)]
68. Shi, M.; Wan, F.; Mao, Y.; Gao, H. Unraveling the mechanism for the viability deficiency of null mutant. *J. Bacteriol.* **2015**, *197*, 2179–2189. [[CrossRef](#)]
69. Sun, L.; Jin, M.; Ding, W.; Yuan, J.; Kelly, J.; Gao, H. Posttranslational modification of flagellin FlaB in *Shewanella oneidensis*. *J. Bacteriol.* **2013**, *195*, 2550–2561. [[CrossRef](#)]
70. Sivaraman, T.; Kumar, T.; Jayaraman, G.; Yu, C. The mechanism of 2, 2, 2-trichloroacetic acid-induced protein precipitation. *J. Protein Chem.* **1997**, *16*, 291–297. [[CrossRef](#)]
71. Meng, Q.; Liang, H.; Gao, H. Roles of multiple KASIII homologues of *Shewanella oneidensis* in initiation of fatty acid synthesis and in cerulenin resistance. *Biochim. Biophys. Acta Mol. Cell Biol. Lipids* **2018**, *1863*, 1153–1163. [[CrossRef](#)]
72. Mirelman, D.; Yashouv-Gan, Y.; Schwarz, U. Peptidoglycan biosynthesis in a thermosensitive division mutant of *Escherichia coli*. *Biochemistry* **1976**, *15*, 1781–1790. [[CrossRef](#)]
73. Thomas, P.E.; Ryan, D.; Levin, W. An improved staining procedure for the detection of the peroxidase activity of cytochrome P-450 on sodium dodecyl sulfate polyacrylamide gels. *Anal. Biochem.* **1976**, *75*, 168–176. [[CrossRef](#)]
74. Liang, H.; Zhang, Y.; Wang, S.; Gao, H. Mutual interplay between ArcA and  $\sigma^E$  orchestrates envelope stress response in *Shewanella oneidensis*. *Environ. Microbiol.* **2021**, *23*, 652–668. [[CrossRef](#)]
75. Fu, H.; Jin, M.; Ju, L.; Mao, Y.; Gao, H. Evidence for function overlapping of CymA and the cytochrome *bc*<sub>1</sub> complex in the *Shewanella oneidensis* nitrate and nitrite respiration. *Environ. Microbiol.* **2014**, *16*, 3181–3195. [[CrossRef](#)] [[PubMed](#)]
76. Schneider, C.A.; Rasband, W.S.; Eliceiri, K.W. NIH Image to ImageJ: 25 years of image analysis. *Nat. Methods* **2012**, *9*, 671–675. [[CrossRef](#)] [[PubMed](#)]
77. Liu, L.; Feng, X.; Wang, W.; Chen, Y.; Chen, Z.; Gao, H. Free rather than total iron content is critically linked to the Fur physiology in *Shewanella oneidensis*. *Front. Microbiol.* **2020**, *11*, 593246. [[CrossRef](#)] [[PubMed](#)]